Journal of Applied Pharmaceutical Science Vol. 15(02), pp 127-141, February, 2025
Available online at http://www.japsonline.com
DOI: 10.7324/JAPS.2025.206829
ISSN 2231-3354

# Development and evaluation of remdesivir dry powder inhalation formulation by spray drying technique

Mukesh Pandurang Ratnaparkhi*, Gajanan Madhukar Kulkarni, Shailendra S. Salvankar, Avinash Ramrao Tekade

Department of Pharmaceutics, Marathwada Mitra Mandal's College of Pharmacy, Thergaon, Maharashtra, India.

**ARTICLE HISTORY**

Received on: 23/06/2024
Accepted on: 16/10/2024
Available Online: 05/01/2025

***Key words:***
Dry powder inhalation, mucoadhesion, pulmonary drug delivery, remdesivir, respiratory viruses, spray drying.

**ABSTRACT**

Remdesivir is an antiviral drug that has broad activity against members of the filovirus, Coronaviruses, and paramyxovirus. After oral administration, it is highly metabolized in the liver resulting in low bioavailability. On the other hand, parenteral administration has systemic side effects. Therefore, in this study, an effort has been undertaken to develop the remdesivir mucoadhesive dry powder inhalation (DPI) formulation by spray drying technique targeting the lung for immediate onset of action and to reduce the side effects of remdesivir associated with parenteral administration. The feed solution was prepared by dissolving a sufficient amount of the drug with Lactose, Leucine, B-cyclodextrin, and a novel mucoadhesive agent (Samanea saman seed gum) at different concentrations in a solvent system of ethanol: water (50:50 v/v) with the help of sonication. After that spray drying process was performed employing a spray dryer. All DPI formulations showed a geometrical size ranging from 3 to 4.8 µm and a polydispersity index less than 0.5. The raw remdesivir showed rectangular-shaped particles, whereas the optimized DPI formulation showed irregular morphology with a rough exterior. Differential scanning calorimetry (DSC) and X-ray powder diffraction study illustrated that the spray drying process changed the crystallinity of the drug as well as other excipients by converting them into the amorphous form. Thereby, increasing the solubility of remdesivir in DPI formulations by about 15–18 times higher than that of plain remdesivir. The amorphous form likely dissolves more quickly than the crystalline form due to stronger intermolecular forces in the crystal and its higher free energy. The drug content and drug release (at the end of 5 hours in phosphate buffer solution (PBS) with a constant temperature of 37°C ± 1°C) were found to be 89.73% ± 2.17% and 79.4% ± 2.2%, respectively. The optimal DPI formulation exhibited excellent aerodynamic performance with 43.583% fine particle fraction and 2.13 µm mass median aerodynamic diameter. Formulated DPI represented a promising strategy for administering remdesivir via the pulmonary route for localized action against pulmonary viral infections.

## INTRODUCTION

Respiratory viruses stand as the predominant pathogens responsible for illnesses in the human population, exerting a substantial influence on global rates of morbidity and mortality, with a particular emphasis on the vulnerable demographic of children [1]. Human respiratory viruses, namely human respiratory syncytial virus, human parainfluenza virus, human rhinovirus, adenovirus (ADV), human coronavirus, human metapneumovirus, human bocavirus, and pharyngoconjunctival fever, widely spread throughout many age groups and are listed for their capacity to transmit effectively from person to person [2,3]. Additionally, in recent years, the severe acute respiratory syndrome coronavirus (SARS-CoV) and avian influenza virus H5N1 have arisen as concerns for global health. Currently, only a limited number of preventive or therapeutic measures are available for treating respiratory viruses, which is why they contribute significantly to the burden of diseases. However, the recent progress in molecular and cellular research pertaining to respiratory viruses holds promise for the discovery of valuable interventions. During one such development, Gilead Sciences discovered a compound via

*Corresponding Author
*Mukesh Pandurang Ratnaparkhi, Department of Pharmaceutics, Marathwada Mitra Mandal's College of Pharmacy, Thergaon, India.*
*E-mail: mukeshparkhi @ yahoo.co.in*

screening unique compound databases for its anti-Ebola virus (EBOV) properties. Subsequent studies have demonstrated its remarkable effectiveness in combating EBOV within HeLa and human umbilical vein endothelial cells [4]. Further, the identified compound has been named as remdesivir.

Remdesivir functions as a wide-ranging antiviral medication [5]. It operates as a monophosphoramide prodrug, undergoing intracellular transformation into an adenosine analog which is processed within the host's system to produce the active nucleoside triphosphate [6,7]. The adenosine nucleoside analog has the capacity to hinder viral RNA polymerases, avoid detection by viral exonucleases, and consequently, reduce viral RNA synthesis [6]. Prior research has shown that remdesivir exhibits wide-spectrum effectiveness against various members of the filovirus (e.g., EBOV, Marburg virus) [8], Coronaviruses (CoVs) (e.g., SARS-CoV, Coronavirus associated with Middle East Respiratory Syndrome) [9,10], and paramyxovirus (e.g., respiratory syncytial virus, Nipah virus, and Hendra virus) [5].

The ease of administering remdesivir through various delivery methods, such as intravenous (i.v.) injection, intramuscular (i.m.) injection, and oral administration, has been thoroughly examined. In the end, it was determined that oral delivery of remdesivir is not feasible due to the extensive first-pass metabolism that significantly metabolizes and rapidly eliminates the drug [11]. This leads to inadequate hepatic stability and low bioavailability, rendering it unsuitable for oral administration. The slow-acting nature of remdesivir's active component in peripheral blood mononuclear cells and its inconsistent release from muscle provide further challenges for its intramuscular (i.m.) administration. Hence, intravenous (i.v.) injection is the chosen route of administration for remdesivir, as it can efficiently access a wide range of tissues, such as the kidney, renal medulla, and liver. However, the intravenous dosage forms are exclusively accessible to patients while they are in a hospital setting which is not convenient, may show hepatotoxicity, there is less patient compliance, and other potential side effects due to the exposure of the drug to other organs [12]. Therefore, the inhalation route emerges as a highly appealing approach for drug administration, enabling the direct transport of medications to the intended site without undergoing first-pass metabolism. Consequently, it has the potential to enhance local antiviral effectiveness within the lungs while limiting systemic side effects. Moreover, less dose is required to administer by inhalation compared to injectable forms [13]. Vermillion *et al.* [14] conducted an efficacy study using repeated doses of inhaled remdesivir in a SARS-CoV-2-infected African green monkey model. The study showed reduced viral replication in both bronchoalveolar lavage fluid and respiratory tissues when compared to a placebo. The efficacy of inhaled remdesivir, administered once daily at a pulmonary deposited dose of 0.35 mg/kg approximately 8 hours after infection, was comparable to that of intravenous remdesivir, which was given as a single 10 mg/kg dose followed by 5 mg/kg daily [14]. In a previous study by Zhang *et al.* [15], the aerosol formulation of R-salbutamol sulfate showed equivalent potent anti-asthmatic effects to the racemic salbutamol formulation, despite requiring only half the dose when administered by inhalation to guinea pigs [15].

The alveolar epithelium is thin and easily permeable with high vasculature, allowing rapid absorption of molecules across the membrane which enables the high and quick absorption of soluble and permeable molecules. Substances with poor absorption rates can be relatively well absorbed following pulmonary administration because the alveolar environment has minimal extracellular and intracellular enzyme activity [16]. Nguyen *et al.* [17] developed a carrier-free sildenafil DPI and assessed its drug transport efficiency using Calu-3 cell lines, which are human airway epithelial cells. Their study revealed that apical-to-basolateral transport showed higher apparent permeability compared to basolateral-to-apical transport, suggesting that pulmonary delivery is an effective method for sildenafil absorption [17]. The essential factor in all inhalation dosage forms, whether they are metered dose inhalers (MDI) or dry powder inhalers (DPI), lies in the requirement to produce the ideal "respirable dose" comprising particles smaller than 5 µm. This optimal dosage ensures the effective delivery of the therapeutic agent to its target site, which is the lungs. This represents a pivotal aspect of performance in the logical development and choice of a pulmonary drug delivery system [18]. There are several advantages of DPI over MDI, such as DPI does not contain any volatile propellant, proper dispersion, and entrainment of the drug particles, portable, rapid onset of action, improved stability of the drug, ease of handling and administration, targeted drug delivery and relatively inexpensive in comparison to the other delivery systems [19]. Recently, Woodcock *et al*. [20] conducted a study comparing the impact of switching from pMDIs to DPIs for maintenance therapy, versus continuing with standard care, on both greenhouse gas emissions and asthma control. The results showed that the group using the fluticasone furoate/vilanterol DPI reduced their inhaler-related carbon footprint by more than half, while consistently achieving better asthma control over a 12-month period compared to those receiving usual care [20].

The spray drying technique was used to produce dry powder as spray-dried powder serves as an appropriate pharmaceutical formulation for the administration of pharmaceutical substances via inhalation [21]. Also, the spray drying technique provides advantages such as a one-step method, rapid, reproducible, and scalable. Furthermore, it allows for control over particle size, shape, crystallinity, and structure by adjusting parameters like the drying gas temperature, the characteristics of the feed solution, and the feeding rate [19]. A solvent evaporation system is well-suited for transforming a liquid solution, suspension, or emulsion into precisely sized and shaped dry powder particles measuring less than 5 µm. These particles can be seamlessly and effectively directed into the lower portion of the respiratory tract [22]. Meanwhile, this method has one limitation when used with stable crystalline drugs, as it primarily generates amorphous particles that are susceptible to moisture and, as a result, are less physically stable [23]. In the present work, the novel mucoadhesive agent Samanea saman gum was introduced for the first time into DPI formulation to increase the residence time of the drug at the site of action to avoid rapid clearance of administered dry powder particles due to the mucociliary as well as alveolar clearance mechanisms. The Samanea saman gum was extracted from the seeds of the Samanea saman plant.

This extraction method is simple, and the gum is not only edible and biodegradable but also non-toxic, readily available, compatible, and cost-effective. Due to its beneficial properties, including a high swelling index, low viscosity, and substantial water retention capacity, it was utilized as a mucoadhesive agent [24,25]. Additionally, lactose was used as a drug carrier, L-leucine was added to enhance both targeting efficiency and dispersibility, and beta-cyclodextrin was included to increase the solubility of remdesivir. Considering the advantages of DPI and the requirement for an effective pulmonary delivery system for remdesivir, an attempt has been made to develop the remdesivir mucoadhesive DPI by spray drying technique. This approach aims to target the lungs for immediate onset of action with increasing residence time and to reduce the side effects of remdesivir associated with parenteral administration. The study primarily evaluates the prepared DPI for solubility, *in-vitro* drug release, aerodynamic properties, stability, and other essential DPI evaluation parameters, which will contribute to achieving the study's objectives.

## MATERIALS AND METHODS

### Materials

API remdesivir was received as a gift sample from Mylan R & D Centre (Bommasandra-jigani Link Road, Bandenallasandra, Bangalore, India). Lactose and L-leucine were purchased from Loba Chemie Pvt. Ltd., Mumbai. Beta Cyclodextrin was procured from Research Lab Fine Chem Industries, Islampur, India. The seeds of Samanea saman were acquired from the Pune city marketplace and the mucoadhesive gum extraction took place in our laboratory. HPLC-grade methanol and acetonitrile, along with distilled water, were employed in the process. All other chemicals used were of reagent grade.

### Methods

#### *Extraction of mucoadhesive agent (Samanea saman seed gum)*

The seeds of Samanea saman were subjected to size reduction utilizing an appropriate method, resulting in a powdered form. Subsequently, the powdered gum was immersed in water for 24 hours to generate a mucilaginous mass [26]. The dispersion underwent gravity filtration, followed by an ethanol treatment to facilitate complete precipitation of the gum. The gum that was precipitated subjected to a drying process at 40°C utilizing a hot air oven to remove any remaining traces of ethanol. Additionally, in order to eliminate any residual ethanol, the desiccated gum underwent pulverization using a mortar and pestle, followed by another round of drying in the oven. Subsequently, it was safeguarded in a dry environment for future utilization [24,25,27,25,27,28].

#### *Characterization of mucoadhesive gum [25,29]*

*Swelling index*

The initial powder volume was documented by weighing 1 g of gum in a 100 ml measuring vessel. Subsequently, the gum was effectively dispersed in distilled water and agitated vigorously. The measuring vessel was kept under ambient conditions for a duration of 24 hours. Following this period, the volume of the gum sediment was recorded. The swelling index was calculated using the subsequent formula (1):

$$\text{Swelling index} = \left[\left(\frac{X_1 - X_0}{X_0}\right)\right] \times 100 \quad (1)$$

Here $X_0$ represents the powder's initial height within the graduated vessel and $X_1$ signifies the height of the swollen gum after 24-hour period.

*Water retention capacity*

After conducting the swelling index study, the material within the measuring vessel underwent filtration utilizing a muslin cloth. Next, the water was fully drained into a 100 ml measuring vessel and its volume was noted [30,31]. The determination of water retention capacity was carried out employing the given expression (2):

$$\text{Water retention(WR)}\ \% = \left[\left(\frac{W_1 - W_0}{W_0}\right)\right] \times 100 \quad (2)$$

Where WR % is the percent water retained, $W_0$ represents the initial weight, while $W_1$ denotes the weight following water retention.

*Viscosity measurement*

The viscosity of a 1% w/v aqueous solution of Samanea saman seed gum was measured utilizing a Brookfield viscometer (DV–1 Prime, Medi Equip, India) at 50 rpm and a temperature of 30°C, applying a torque of 6.9% [32,33].

*Hydration capacity*

Precisely measuring 1 g of powdered gum, then it was deposited into a 15 ml centrifugation tube. Subsequently, filled with 10 ml of distilled water, and the resulting mixture underwent centrifugation at 1,500 rpm for 15 minutes at room temperature. The supernatant was extracted from the centrifuge by inverting the tared tube. Subsequently, a digital balance was employed to measure the weight of the decanted tube [34]. The hydration capacity was calculated by employing the following expression (3):

$$\text{Hydration capacity} = \frac{\text{Weight of hydrated sample}}{\text{Weight of dry sample}} \quad (3)$$

*Moisture sorption capacity*

A precisely measured quantity of 1 g (Initial weight) of powdered gum was evenly distributed within a petri dish and placed in a programmable humidity chamber, where it was kept at a temperature of 37°C ± 1°C and a relative humidity of 100% for a duration of 2 days. The moisture sorption capacity was determined through the comparison of sample weights prior to and following the assessment [35,36].

#### *Design of experiment*

A three-factor two-level ($2^3$) factorial design was utilized to outline different formulation batches [37]. The ratio

of drug and lactose, amount of beta-cyclodextrin, and percent mucoadhesive agent were chosen as formulation variables. They were studied at two levels (i.e., High and low). All other formulation and processing variables such as the amount of Leucine (800 mg) and solvent system—ethanol: water (50:50 v/v) were kept constant in all the prepared batches. Table 1 presents a summary of the 8 experimental runs investigated. Particle size (Y1), Polydispersity Index (PDI) (Y2), Drug content (%) (Y3), and Drug release (%) (Y4), were considered in the study as response parameters. The experimental design was prepared by employing the Design Expert® software (version 8.0.7.1; M/s Stat-Ease Inc., Minneapolis, USA).

### *Method of preparation of mucoadhesive remdesivir dry powder for inhalation*

Remdesivir dry powder was prepared by using spray drying technique [37]. Different dry powder inhalation (DPI) formulations were produced in triplicate using $2^3$ factorial designs as shown in Table 1. In brief, Feed solution was prepared by dissolving a sufficient amount of drug with Lactose, Leucine, B-cyclodextrin, and mucoadhesive agent at different concentrations in a solvent system of ethanol and water with the help of sonication. After that Spray drying process was performed employing a spray dryer (LU222, VCX–750, Labultima, India) using a standard 0.7 mm nozzle. The spray drying conditions were maintained at an Inlet temperature of 130°C & outlet temperature of 100°C. The dispersion was introduced into the nozzle through a peristaltic pump at a feeding rate of 1 ml/minute. It was subsequently atomized through the application of compressed air pressure and then co-delivered with heated air into the drying compartment. The dried powder was harvested from the apparatus collecting chambers [38].

## Characterization of mucoadhesive remdesivir dry powder for inhalation

### *Particle size and PDI*

The particle size and PDI were assessed using a particle size analyzer employing the dynamic light scattering technique. In this procedure, 1 mg of the powdered sample was dispersed in a 20 ml volume of glycerol. Subsequently, the mixture underwent ultrasonic agitation for a duration of 2 minutes, and the measurements were taken utilizing a Zetasizer (Malvern, UK) [39].

**Table 1.** Independent variables in remdesivir DPI formulation from $2^3$ factorial design.

| Formulation code | Drug : Lactose | B-cyclodextrin (mg) | Mucoadhesive agent (%) |
|---|---|---|---|
| F1 | 1 : 6 | 600 | 2.5 |
| F2 | 1 : 6 | 600 | 5 |
| F3 | 1 : 8 | 600 | 2.5 |
| F4 | 1 : 8 | 600 | 5 |
| F5 | 1 : 8 | 400 | 5 |
| F6 | 1 : 8 | 400 | 2.5 |
| F7 | 1 : 6 | 400 | 2.5 |
| F8 | 1 : 6 | 400 | 5 |

### *Percentage yield*

The practical yield was assessed from the direct measurement of powder obtained from the spray dryer units cyclon 1 and cyclon 2. The theoretical yield was the amount of powder mixture subjected to the spray drying process [40,41]. The percentage yield of each formulated batch was calculated by utilizing the following expression:

$$\text{Percentage yield} = \frac{\text{Practical yield}}{\text{Theoretical yield}} \times 100 \quad (4)$$

### *Scanning electron microscopy (SEM)*

The morphology of both the raw remdesivir and prepared DPI formulation was assessed using SEM. A minute quantity of the powdered sample was positioned on a carbon tape, and a sputter coater was employed to apply a coating to the sample before capturing the images. The images were obtained utilizing a field emission scanning electron microscope (FEI Nova Nano SEM 450) [42].

### *Fourier-transform infrared spectroscopy (FTIR)*

FTIR spectra of raw Remdesivir, Lactose, Leucine, B-cyclodextrin, mucoadhesive agent, and the optimized DPI formulation were acquired using an FTIR instrument (Alpha-1, 8,400 IR Affinity 1-CE, Shimadzu, Japan). The scanning span ranged from 450 to 4,000 $cm^{-1}$ employing a resolution of 1 $cm^{-1}$. The sample chamber was cleansed with ethanol and configured for background clearance. Subsequently, the sample was positioned in the sample chamber, and the swivel pressure tower was affixed before proceeding with the sample analysis [43].

### *Differential scanning calorimetry (DSC)*

The thermal analysis of the drug, Lactose, Leucine, B-cyclodextrin, mucoadhesive agent, and optimized remdesivir dry powder was performed by utilizing a DSC (Mettler Toledo, USA). The sample was weighed 3–8 mg and filled into the bottom pan after that lead was placed over it followed by hermetical sealing. The heating range was 30°C–350°C with continuous elevation of temperature maintained at a rate of 10°C per minute within a nitrogen atmosphere (50–60 ml/minute). The prepared sample was placed inside the sample chamber and heated over the above-mentioned heating range [44,45].

### *X-ray powder diffraction (XRPD)*

The crystallinity of the formulated dry powder of remdesivir and other excipients was evaluated using an X-ray diffraction instrument (BRUKER D8 VENTURE) consisting of a primary monochromated radiation and filter (K-beta filter). The equipment was utilized with an accelerating voltage of 40 kV at 40 mA. Specimens were ground using mortar and pestle and powder was placed into the sample compartment till a predefined level and subjected to continuous scanning at a

scanning speed of 10.0000 deg/minute and the scan range was 5.0000–60.0000 deg [46].

***Solubility study***

The solubility of plain remdesivir and remdesivir in DPI formulations was assessed in phosphate buffer (pH 7.4). The excess amount of powder was added to phosphate buffer pH 7.4 until precipitation occurred. The samples were agitated using an orbital shaker at 250 revolutions per minute and maintained at a temperature of 25°C for a duration of 24 hours. Following this incubation, the samples were harvested and subsequently subjected to centrifugation at 15,000 rpm for a period of 15 minutes. Following centrifugation, the supernatants were gathered and analyzed by Ultraviolet (UV) spectrophotometer with a wavelength set at 246 nm [31].

***Drug content***

The content of remdesivir in DPI formulations was assessed by employing a UV spectrophotometer, with measurements conducted at a wavelength of 246 nm. The prepared powder formulations were diluted using PBS pH 7.4 before analysis by UV spectrophotometer [47]. The drug content was measured using the given expression:

$$\text{Drug content \%} = \frac{\text{Actual amount of drug}}{\text{Theoretical amount of drug}} \times 100 \qquad (5)$$

***In vitro diffusion study***

Drug release from the formulated remdesivir DPI was investigated *in vitro* using Franz diffusion cells. In this experimental setup, a dialysis membrane separated the donor compartment, which held the dry powder, from the receptor compartment which was loaded with a PBS (pH of 7.4). The temperature was consistently kept at 37°C ± 1°C through the use of a circulating water bath, maintaining a stable experimental environment. Samples were periodically collected at time points of 15, 30, 60, 90, 120, 150, 180, 240, and 300 minutes from the receptor compartment. Each time, they were substituted with an equivalent volume of freshly pre-heated buffer solution and subsequently analyzed using a UV spectrophotometer at a wavelength of 246 nm [48].

***Study of aerodynamic property using a cascade impactor***

The aerodynamic diameter distribution of the formulated DPI was evaluated using an 8-stage Andersen Cascade Impactor (ACI). The ACI segregates the sample into fractions based on inertial impaction principles. A measured quantity of powder equivalent to 5 mg of remdesivir was encapsulated within a size #3 HPMC hard capsule and then inserted into the Rotahaler®. Afterward, the powder was dispensed into the impactor at a flow rate of 60 l/minute for 5 seconds per actuation, resulting in a 4 kPa pressure drop across the device. The drugs were recovered from the capsule, induction port, inhaler device, mouthpiece adaptor, and ACI stages with collection plates through a procedure involving the rinsing of each component with 10 ml of dimethyl sulfoxide. The analysis of the amount of drug at each stage was determined by HPLC (LC 100, Cyberlab model with LC-10 software consisting of LC-20AT pump, UV/Visible detector (SPD 20 A), and 20 µl Hamilton syringe). It was performed via C18 column (250 × 4.6 mm, 3.5 µm) in isocratic elution mode, and acetonitrile: methanol (50:50 v/v) was used as mobile phase at a flow rate of 0.7 ml/minute. The analysis was carried out at a wavelength of 246 nm, utilizing a 12-minute runtime. The mobile phase was freshly prepared and subjected to 5 minutes of sonication to remove any dissolved gases. Both the column and the HPLC system were kept at room temperature. The mass median aerodynamic diameter (MMAD), fine particle fraction % (FPF %), and geometric standard deviation (GSD) were determined using a log-probit plot [49].

***Stability study***

The stability investigation adhered to the ICH guidelines was conducted in order to assess the stability of the optimized batch of remdesivir mucoadhesive DPI. The samples were maintained at a temperature of 40°C ± 0.5°C and a relative humidity of 75% ± 5% for a duration of 3 months. Following this timeframe, the specimens were retrieved and systematically analyzed at regular intervals for physical attributes, particle size, PDI, drug content, and *in vitro* drug release, in accordance with predetermined time points.

## RESULTS AND DISCUSSION

**Characterization of mucoadhesive gum**

The outcomes obtained from the analysis of mucoadhesive gum are presented in Table 2. The sample's final weight, after completing the moisture sorption capacity test, was determined to be 1.0527 ± 0.0061 g. The gum exhibits a significant capacity for water retention and maintains a low viscosity. The amount of water retained in the gum plays a crucial role in establishing its hydrophilic nature. The low viscosity of gum renders it a preferred option for getting better solubility and bioavailability of drugs that exhibit limited water solubility [25]. Due to the expansion tendency of the gum, its surface area undergoes enlargement upon dissolution, thereby substantially enhancing the rate at which the drug dissolves and also helps in retaining at the site of action for a longer period of time due to better adhesion to the mucosal linings.

**Table 2.** Characterization of mucoadhesive gum.

| Parameters | Samanea saman seed gum |
|---|---|
| Colour | Brownish to Pale white |
| pH | 5.3 ± 0.010 |
| Solubility | Form colloidal solution in water and insoluble in alcohol, chloroform, and ethanol |
| Swelling index (%) | 22.22 ± 2.87 |
| Water retention capacity (ml) | 2 ± 0.020 |
| Viscosity (cps) | 2.40 ± 0.16 |
| Hydration capacity (w/w) | 1.029 ± 0.018 |
| Moisture sorption capacity (%) | 5.27 ± 0.61 |

Each value represents mean ± SD ($n$ = 3).

**Characterization of mucoadhesive remdesivir dry powder for inhalation**

***Particle size and PDI***

Particle size distribution and PDI for all 8 formulated batches were assessed utilizing a particle size analyzer with a dynamic light scattering technique. The particle size and size distributions have been compiled in Table 3. It is noteworthy that all DPI formulations exhibited a geometric size within the range of 3–4.8 µm which can be considered a suitable particle size for inhalation therapy and drug particles may retain in the upper as well as middle part of the respiratory tract. Overall, it would be a favourable particle size for treating localized pulmonary viral infections. The particle size of formulation F3 (3.642 ± 0.193 µm) was found to be most appropriate as per the requirement of treatment and also had the smallest PDI compared to the other formulated batches. It is evident that spray drying led to a narrower and more symmetrical particle size distribution which was below 0.5 PDI indicating nearly monodispersible powder however there may be the inclusion of a smaller population of multiple particle sizes [50]. Furthermore, the incorporation of leucine into the formulation did not produce any alterations in the particle size but changing the percentage of mucoadhesive agent had shown a significant effect on the particle size. When the percentage of mucoadhesive agent was increased, their particle size also increased (Fig. 8).

***Percentage yield***

The percentage yield of each formulated batch was measured and is given in Table 3. A higher percentage of yield was obtained for the F3 batch of remdesivir DPI formulation due to the greater amount of lactose. The lactose acts as a drug carrier and also enhances the targeting efficiency.

***Scanning electron microscopy***

As indicated by SEM images presented in Figures 1 and 2, the raw Remdesivir showed rectangular-shaped particles whereas the optimized DPI formulation showed an irregular morphology with a rough exterior. The textured appearance of these particles could be attributed to the swift evaporation of ethanol within the spray drying chamber. Initially, spherical droplets, formed when the solution was sprayed, underwent a reduction in size as a consequence of the rapid dissipation of ethanol vapor from their inner core. The presence of a corrugated surface structure has been identified as a means to improve the aerodynamic efficiency of particles through an elevation in the dynamic shape factor coefficient. While the overall surface area of a corrugated particle may be substantial, numerous regions are concealed by its irregularities. Consequently, the effective area accessible for interaction with adjacent particles becomes constrained, leading to a reduction in powder cohesion and an enhancement in the powder's dispersion into aerosol.

**Table 3.** Particle size, PDI and percentage yield of remdesivir mucoadhesive DPI formulations.

| Formulation | Particle size (um) | Polydispersity index | Percentage yield (%) |
|---|---|---|---|
| F1 | 3.051 ± 0.148 | 0.3951 ± 0.0211 | 47.66 |
| F2 | 4.398 ± 0.122 | 0.4532 ± 0.0266 | 54.28 |
| F3 | 3.642 ± 0.193 | 0.2657 ± 0.0169 | 57.82 |
| F4 | 4.715 ± 0.212 | 0.4766 ± 0.0348 | 56.77 |
| F5 | 4.123 ± 0.187 | 0.4828 ± 0.0421 | 55.08 |
| F6 | 4.093 ± 0.256 | 0.2607 ± 0.0234 | 45.77 |
| F7 | 4.048 ± 0.152 | 0.3421 ± 0.0355 | 51.48 |
| F8 | 4.317 ± 0.232 | 0.4012 ± 0.0272 | 53.42 |

Each value represents mean ± SD ($n$ = 3).

***Fourier-transform infrared spectroscopy***

The FTIR spectrum of remdesivir was taken and the observed peaks are shown in Figure 3 and Table 4. All the functional groups found in the structure of remdesivir were present in the FTIR spectra of the drug which confirmed that the given sample was of remdesivir [51].

Figure 3 illustrates the FTIR spectrum of the optimized batch of DPI. The spectrum showed different characteristics peaks which were similar to peaks found in the Drug and all other excipients. The peak of the C─O group (Fig. 3) was observed in the spectra of the optimized batch of DPI at around 1,029.99 $cm^{-1}$ which corresponded to the C─O stretching of plain remdesivir, lactose, and mucoadhesive agent [52]. The peak of asymmetric stretching vibration of C-O-C was observed in the spectra of the optimized batch of DPI at around 1,114.86 $cm^{-1}$ which was similar to the asymmetric stretching vibration of C-O-C of lactose [53]. The peak of C=C stretching was observed in the spectra of the optimized batch of DPI at around 1,658 $cm^{-1}$ which was identical to the C=C stretching of plain remdesivir. The peak of C─H stretching was observed in the spectra of the optimized batch of DPI at around 2,924.09 $cm^{-1}$ which was similar to the C─H stretching of plain remdesivir, leucine, beta-cyclodextrin, and mucoadhesive agent. The peak of O─H stretching was observed in the spectra of the optimized batch of DPI at around 3,213.41 $cm^{-1}$ which was similar to the O─H stretching of plain remdesivir, lactose, beta-cyclodextrin, and mucoadhesive agent [54]. The peak of N─H stretching was observed in the spectra of the optimized batch of DPI at around 3,423.65 $cm^{-1}$ which was similar to the N─H stretching of plain remdesivir and beta-cyclodextrin [55].

The plain remdesivir FTIR spectra containing peaks of C=C, C─O, C─H, O─H, and N─H stretching were similarly found in the spectra of the optimized batch of DPI as shown in Figure 3. However, the peaks of other excipients were also observed in the spectra of optimized DPI formulation. Therefore, it can be inferred that no chemical interaction occurred between the drug and excipients.

***Differential scanning calorimetry (DSC) study***

DSC is a fundamental technique employed for assessing the crystallinity and amorphous characteristics of a drug within a compound. Here, the sharp endothermic peak of remdesivir was observed at 139.67°C as shown in Figure 4, which indicates that the drug is crystalline in nature and present in the pure form. In the DSC thermogram of the optimized batch

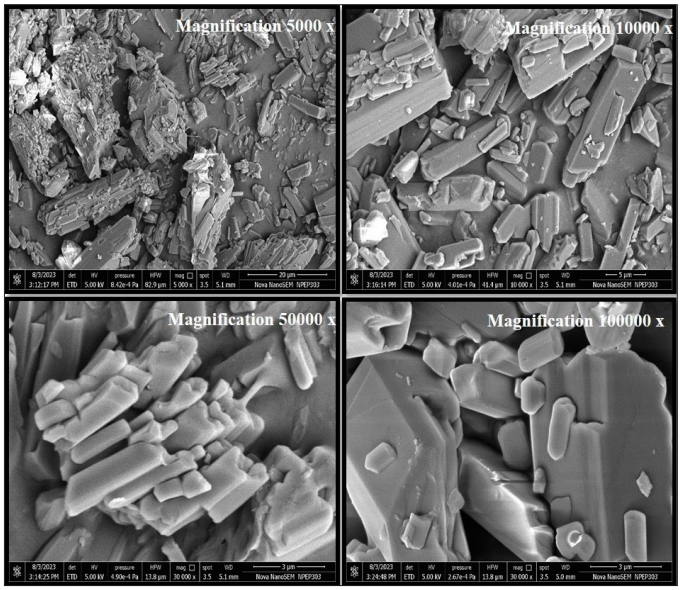


**Figure 1.** SEM images of raw remdesivir at different magnification levels.

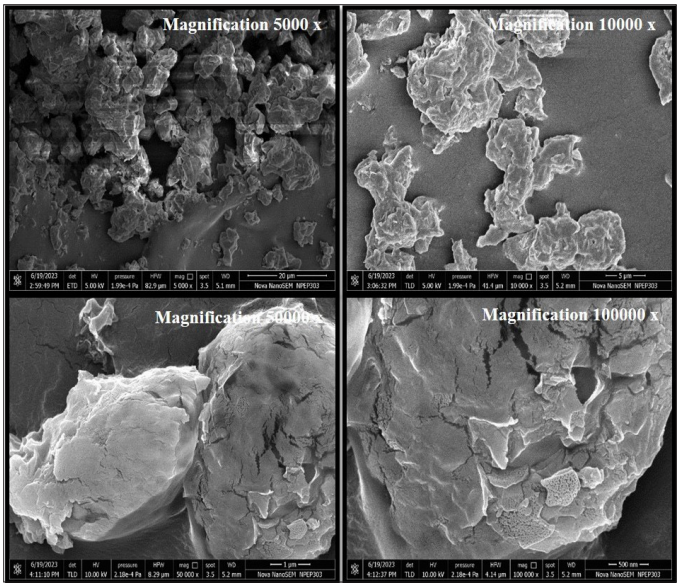


**Figure 2.** SEM images of optimized DPI formulation at different magnification levels.

of DPI, there were three defined endothermic peaks observed at 141.79°C, 162.24°C, and 191.26°C which were attributed to remdesivir, lactose, and mucoadhesive agent, respectively, as shown in Figure 4. In the overlay of the DSC thermogram, the optimized batch of remdesivir DPI shows a smaller peak of the drug as compared to the plain remdesivir which can be considered as there was a change in the nature of the drug from crystalline to amorphous form. However, the disappearance of the peaks corresponding to beta-cyclodextrin and L-leucine in the thermogram of optimized DPI can be attributed to the amorphous structure acquired by beta-cyclodextrin and L-leucine after the spray drying process which was desirable as per the study objectives. The small peak of the mucoadhesive agent was observed which was shifted to a lower temperature. The two peaks of lactose with less intensity were also observed in the optimized DPI formulation. Overall, it can be concluded that the formulation components exhibit thermal stability and are compatible within the temperature range of 30°C–350°C, as no degradation peak was observed in the DSC thermogram.

### *X-ray powder diffraction (XRPD)*

In the diffractogram of remdesivir, several distinct peaks were observed from which the highest peak was detected at two theta degrees of 16.080 with an intensity of 35,339 as shown in Figure 5. Other peaks were also observed at two theta degrees of 8.040, 10.580, 12.640, 16.820, 22.220, and 24.260 with intensities of 3,932, 5,876, 7,367, 10,505, 30,196, and 7,200, respectively. These obtained sharp peaks in the diffractogram (Fig. 5) indicated that the raw remdesivir was crystalline in nature, and these outcomes substantiate the conclusions drawn from the DSC analysis.

In the overlay of the XRPD diffractogram (Fig. 5), the optimized batch of remdesivir DPI showed two very small peaks at two theta degrees of 16.320 and 22.780 with an intensity of 5,281 and 1,580 which were attributed to remdesivir. The intensity of these two peaks decreased massively as compared to peaks in the diffractogram of plain remdesivir which can possibly be happened because of the transformation of remdesivir from crystalline to an amorphous state. The highest peak was detected in the optimized batch of DPI at two theta degrees of 19.960 with an intensity of 14,548 which was similar to a peak of lactose (two theta degrees of 19.980 with an intensity of 81,579) as shown in Figure 5 but there was lowering of the intensity illustrating that the nature of lactose changed from crystalline to amorphous after the spray drying process. Similarly, there were other very small peaks observed in the diffractogram of the optimized batch of DPI as compared to the peaks of raw materials before spray drying demonstrating that the spray drying process changed the crystallinity of the drug as well as other excipients such as lactose and L-leucine by converting them into the amorphous form, and it also support the outcomes of DSC. Recently, some studies obtained crystalline dry powder of remdesivir after using a similar spray-drying technique, whereas our study yielded amorphous dry powder confirmed by XRPD characterization, which is a more desirable outcome for better mucosal adherence [41].

### *Solubility study*

The solubility of plain remdesivir and remdesivir in DPI formulations was conducted in phosphate buffer with a pH of 7.4. The corresponding outcomes are presented in Table 5. The solubility of remdesivir in DPI formulations was about 15–18 times higher compared to plain remdesivir (0.709 ± 0.008 mg/ml *vs*. 0.0403 ± 0.003 mg/ml). The higher solubility of remdesivir found in the F3 and F4 batches were 0.6829 ± 0.014 mg/ml and 0.709 ± 0.008 mg/ml, respectively. The formulations containing a higher amount of beta-cyclodextrin showed higher solubility of remdesivir. Concluding the solubility investigation, it can be inferred that after the spray drying

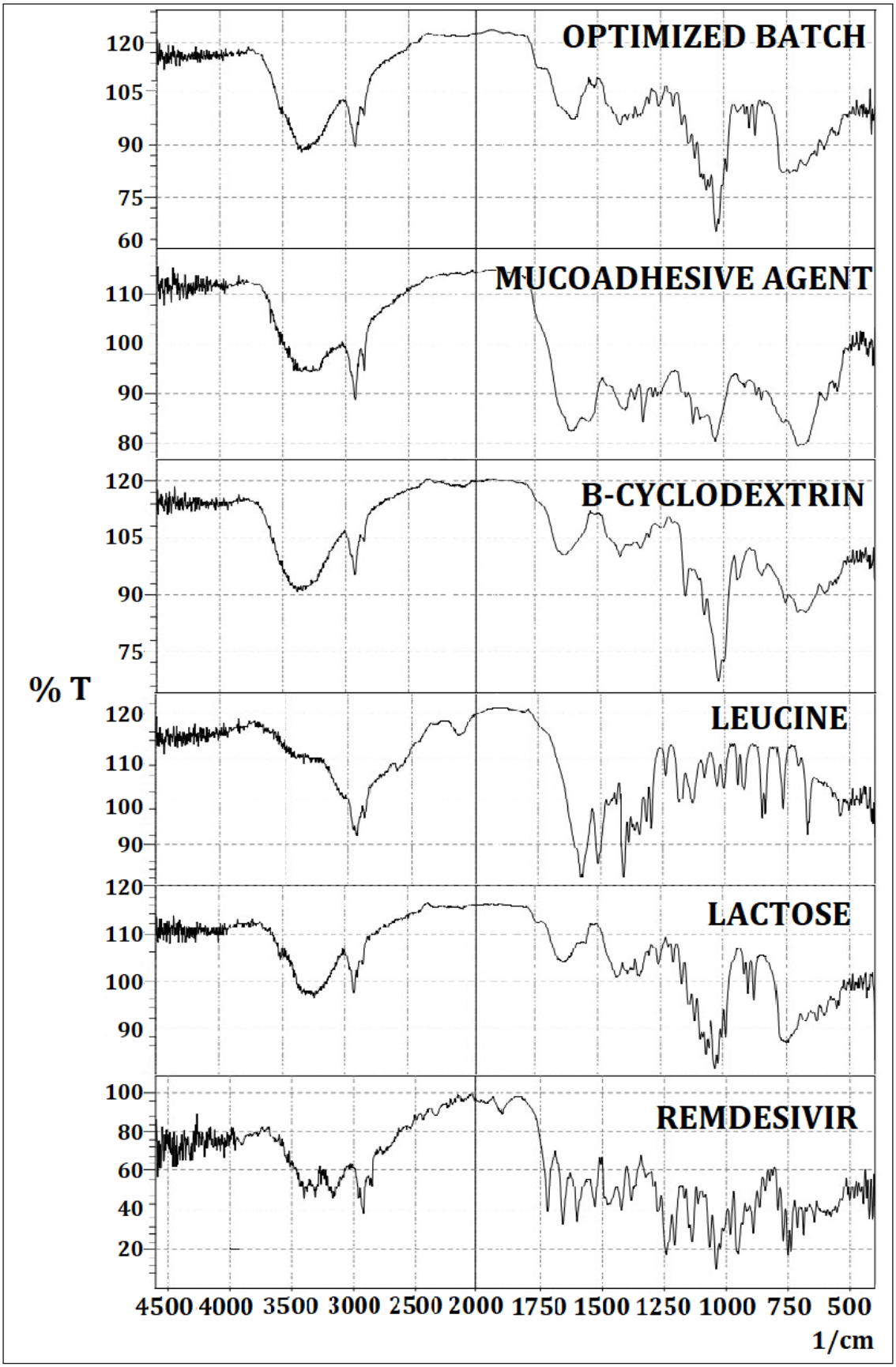


**Figure 3.** FTIR overlay spectra of raw remdesivir, lactose, leucine, B-cyclodextrin, mucoadhesive agent, and optimized DPI formulation.

process, the solubility of remdesivir was increased due to the reduction of particle size, complexation with excipients such as beta-cyclodextrin and also due to the transformation from crystalline state to amorphous state which can be illustrated from the findings of DSC and XRPD studies.

### *Drug content*

The content of remdesivir in DPI formulations was measured by employing a UV spectrophotometer at a wavelength of 246 nm. Table 5 shows the drug content % results of the remdesivir mucoadhesive DPI formulations. The drug content percentage for all eight formulations was observed to exceed 75%, ranging from 76.29% (F2) to 90.7% (F7). According to these findings, it is evident that the formulation with 2.5% mucoadhesive agents (F1, F3, F6, and F7) had a higher average percentage of drug content as compared to the formulation with 5% mucoadhesive agents. The drug content % seems to be slightly dependent on the ratio of drug and lactose. The varying amount of beta-cyclodextrin also does not exhibit any impact on the drug content %.

**Table 4.** Peak and principle groups present in the IR spectrum of remdesivir.

| Sr. No. | Standard value range (cm-) | Observed value (cm- ) | Interpretation (Functional group) |
|---|---|---|---|
| 1. | 1,050–1,150 | 1,138 | C─O group |
| 2. | 1,000–1,350 | 1,242.16 | C─N group |
| 3. | 1,600–1,680 | 1,658.78 | C═C group |
| 4. | 1,640–1,810 | 1,736.23 | C═O group |
| 5. | 2,850–3,000 | 2,960.41 | C─H group |
| 6. | 2,500–3,400 | 3,202.19 | O─H group |
| 7. | 3,300–3,500 | 3,406.17 | N─H group |

### *In vitro diffusion study*

The *in vitro* drug release of formulated remdesivir DPI was conducted utilizing Franz diffusion cells equipped with a dialysis membrane and analyzed by UV spectrophotometer. Figures 6 and 7 show the release profiles of remdesivir mucoadhesive DPI formulations. More than 75% of remdesivir in F3, F4, F5, F6, and F7 was released and dissolved in 300 minutes, whereas 60%–70% of remdesivir in F1, F2, and F8 was released in 300 minutes. These results indicate that the excipients play a role in remdesivir release in a pH medium of 7.4 up to 300 minutes. The excipients mainly include a mucoadhesive agent (Samanea saman seed gum) which causes longer residence of the drug at the membrane and increases release of remdesivir into the phosphate buffer medium (pH 7.4). Spray drying has been reported to modify the size and morphology of particles, ultimately influencing the release profile. Remdesivir mucoadhesive DPI formulations exhibited a reduced release rate during the initial stages and a marginally greater overall drug release at the end of 5 hours (>75%). The release was boosted after 30 minutes which may be due to the time required for saturation of the drug at the membrane.

### *Effect of independent variables on responses and statistical analysis*

The independent variables in the three-factor two-level ($2^3$) factorial design and their recorded responses are presented in Table 6. The optimized batch was assessed based on four responses, Y1 (Particle size), Y2 (PDI), Y3 (Drug content %), and Y4 (Drug release %), and analysis of variance (ANOVA) was performed to check the significance of fitting of experimental data. Formulation F3 was found

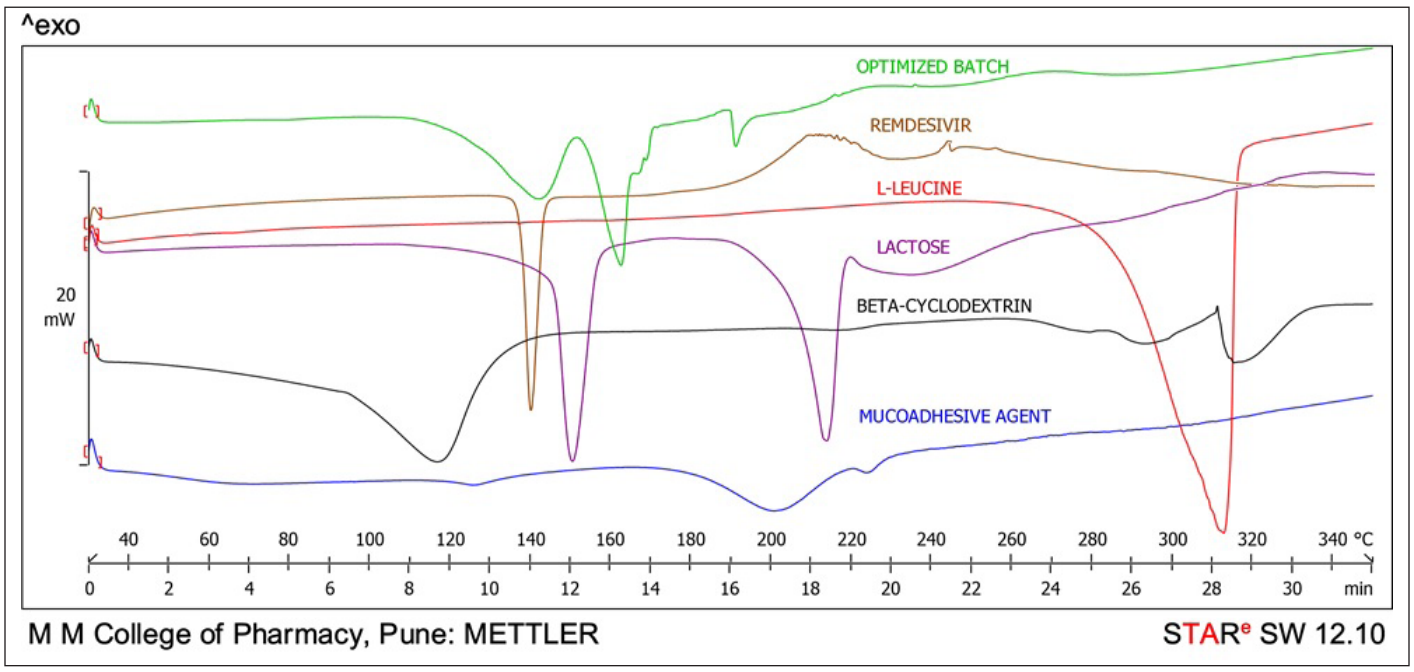


**Figure 4.** DSC thermogram of remdesivir, lactose, leucine, B-cyclodextrin, mucoadhesive agent, and optimized DPI formulation.

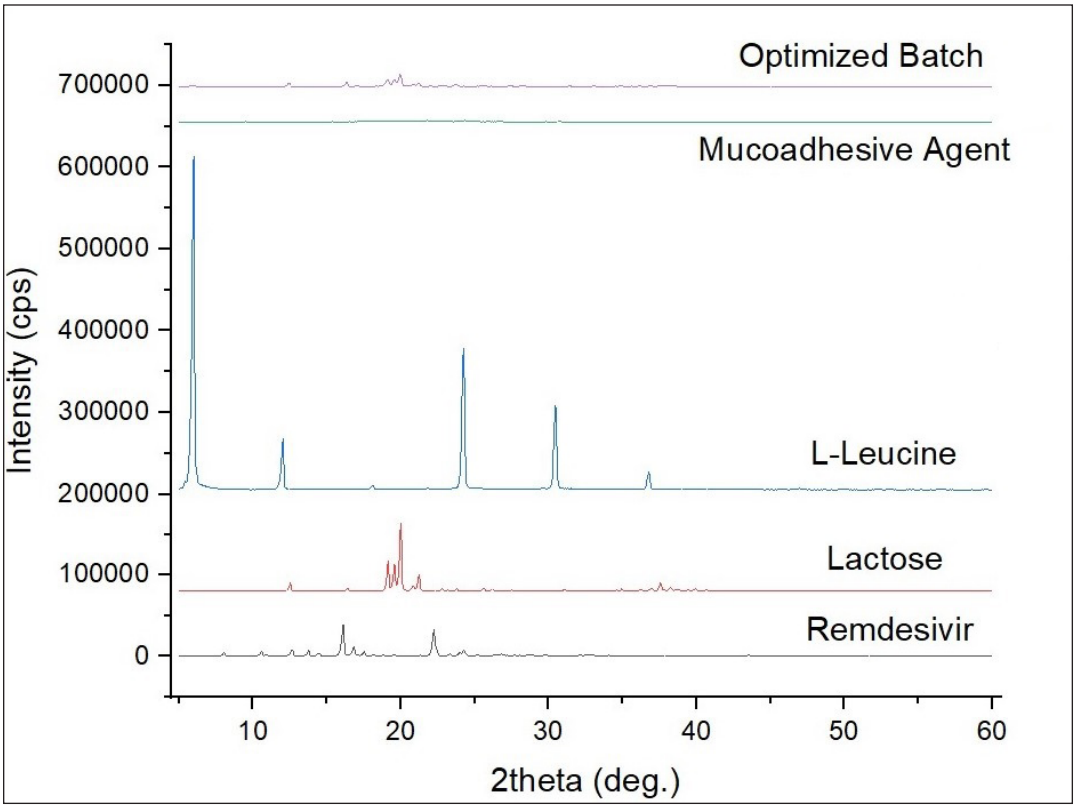


**Figure 5.** X-ray powder diffraction (XRPD) diffractograms of remdesivir, lactose, leucine, mucoadhesive agent, and optimized DPI formulation.

**Table 5.** Solubility data of remdesivir and remdesivir in DPI formulations and drug content %.

| Sample name | Solubility (mg/ml) | Drug content % |
|---|---|---|
| Remdesivir | 0.0,403 ± 0.003 | - |
| F1 | 0.671 ± 0.009 | 86.34 ± 2.75 |
| F2 | 0.4,573 ± 0.012 | 76.29 ± 1.9 |
| F3 | 0.6,829 ± 0.014 | 89.73 ± 2.17 |
| F4 | 0.709 ± 0.008 | 82.15 ± 3.48 |
| F5 | 0.2,103 ± 0.018 | 83.91 ± 3.66 |
| F6 | 0.2,673 ± 0.011 | 88.35 ± 2.89 |
| F7 | 0.4,589 ± 0.016 | 90.7 ± 1.63 |
| F8 | 0.3,978 ± 0.008 | 82.88 ± 2.41 |

Each value represents mean ± SD ($n$ = 3).

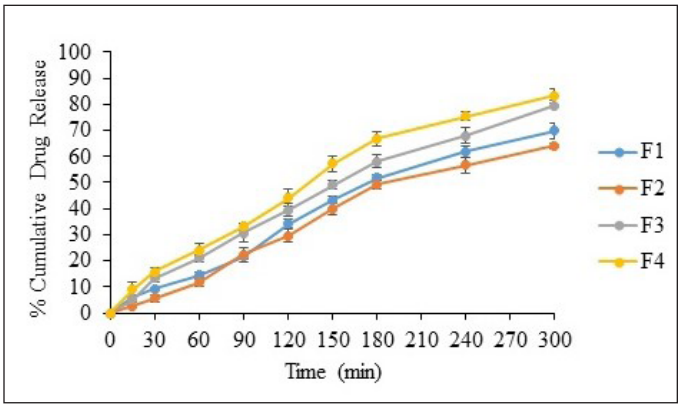


**Figure 6.** *In vitro* percent drug release from F1-F4 [mean ± SD ($n$ = 3)].

to be superior over other formulations, with the desired particle size (between 1 and 5 µm), less PDI (0.2657), high drug content (89.73), and optimum drug release (79.4%). Although formulation F7 yielded the highest drug content (90.7%), the resultant particle size and PDI were not as desired. Similarly, formulation F4 showed the highest drug release (83.2%); however, the resultant particle size, PDI, and drug content were not suitable.

$$\text{Particle size} = 4.05 + 0.0949*A - 0.0969*B + 0.3399*C + 0.1321*AB - 0.0641*AC + 0.2651*BC \quad (6)$$

$$\text{PDI} = 0.3847 - 0.0132*A + 0.0130*B + 0.0688*C - 0.0133*AB + 0.0395*AC - 0.0015*BC \quad (7)$$

$$\text{Drug content} = 85.04 + 0.9912*A - 1.42*B - 3.74*C + 1.32*AB + 0.7313*AC - 0.6712*BC \quad (8)$$

$$\text{Drug release} = 74.44 + 3.96*A - 1.06*B - 0.8125*C + 3.96*AB + 1.51*AC + 1.09*BC \quad (9)$$

The quadratic model is demonstrated to be significant based on the $R^2$ values (Table 7) and $p$-values less than 0.0500. The terms A, B, C, AB, AC, BC, and AC were identified as

significant contributors to the model (Equations 6–9). A three-dimensional response surface plot of particle size revealed that variations in beta-cyclodextrin concentration had an impact on particle size (Fig. 8). A higher concentration of beta-cyclodextrin resulted in smaller particles. This might be because the drug particles complexed with the beta-cyclodextrin, changing their shape from crystalline to amorphous, and the subsequent spray-drying process decreased the size of the particles.

Drug content was shown to be affected by variations in the proportion of mucoadhesive agents in a three-dimensional response surface plot (Fig. 8). The drug content increased as the mucoadhesive agent proportion dropped. However, the beta-cyclodextrin was slightly affecting the drug content as it is not directly involved in the surface phenomenon which generally occurs due to the entrapment of particles or adhesion of particles. The three-dimensional response surface plot of the drug release explains that the higher the amount of mucoadhesive agent, the more time required for the release of the drug because the more availability of gum will retard the drug release, revealing that gum has a property of adhesion, which is desired as per the objectives of the study (Fig. 8).

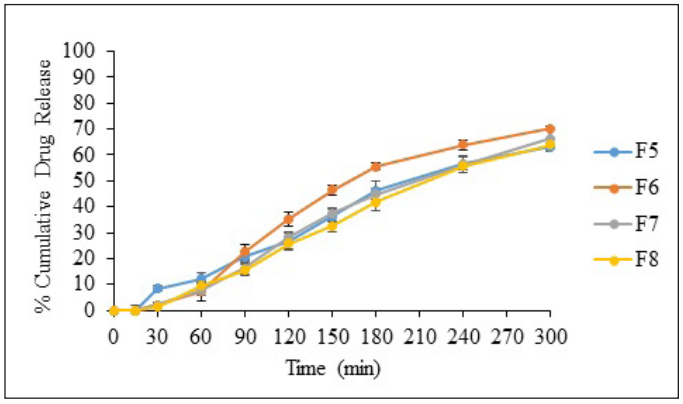


**Figure 7.** *In vitro* percent drug release from F5-F8 [mean ± SD ($n$ = 3)].

***Study of aerodynamic property using a cascade impactor***

The correlation between the particle-size distribution of the administered dose and the delivery efficiency is crucial, as it profoundly impacts the deposition process within the respiratory system. Typically, particles with a diameter exceeding 5 µm are deemed unsuitable for effective pulmonary deposition. For optimal delivery to the deep lung, even finer particles in the range of 2–3 µm may be more favorable [56]. The optimized Remdesivir DPI formulation (F3) had an FPF (<5 µm) of 43.583% and an emitted dose (ED) of 88.98% (Fig. 9), which is higher in contrast to another recent study conducted by Saha *et al.* [39] where they achieved a 72% ED for a single dry powder of remdesivir with an FPF of 55% [38]. The MMAD was found to be 2.13 µm obtained from a log-probit graph with an $R^2$ of 0.938. The obtained MMAD was in between 2 and 3 µm, and therefore, it can be considered as appropriate for targeting the primary and secondary bronchi of the lungs. As we know, viral infections mainly reside in the bronchial region, so it can be concluded that the prepared DPI can be efficient in depositing the drug inside the lungs. However, the MMAD obtained is comparatively lower than that reported in an earlier study, where they observed an MMAD between 4 and 5 µm, indicating the use of superior spray drying

**Table 6.** Effect of independent variables on responses.

| Run | Factor 1 | Factor 2 | Factor 3 | Response 1 | Response 2 | Response 3 | Response 4 |
|---|---|---|---|---|---|---|---|
| | A:Drug : Lactose | B:B-Cyclodextrin | C:Mucoadhesive agent | Particle size | PDI | Drug content | Drug release |
| | | mg | % | um | | % | % |
| F1 | 1:6 | 600 | 2.5 | 3.051 | 0.3,951 | 86.34 | 66.8 |
| F2 | 1:6 | 600 | 5 | 4.398 | 0.4,532 | 76.29 | 64.1 |
| F3 | 1:8 | 600 | 2.5 | 3.642 | 0.2,657 | 89.73 | 79.4 |
| F4 | 1:8 | 600 | 5 | 4.715 | 0.4,766 | 82.15 | 83.2 |
| F5 | 1:8 | 400 | 5 | 4.123 | 0.4,828 | 83.91 | 75 |
| F6 | 1:8 | 400 | 2.5 | 4.093 | 0.2,607 | 88.35 | 76 |
| F7 | 1:6 | 400 | 2.5 | 4.048 | 0.3,421 | 90.7 | 78.8 |
| F8 | 1:6 | 400 | 5 | 4.317 | 0.4,012 | 82.88 | 72.2 |

**Table 7.** Analysis of variance (ANOVA).

| Response | Model fitting | R2 | Adjusted R2 | Predicted R2 | SD | % CV |
|---|---|---|---|---|---|---|
| Particle size | Quadratic | 0.9,999 | 0.9,994 | 0.9,946 | 0.0,124 | 0.3,057 |
| Polydispersity index | Quadratic | 0.9,998 | 0.9,983 | 0.9,847 | 0.0,036 | 0.9,375 |
| Drug content | Quadratic | 0.9,993 | 0.9,954 | 0.9,579 | 0.3,217 | 0.3,783 |
| Drug release | Quadratic | 0.9,997 | 0.9,976 | 0.9,779 | 0.3,182 | 0.4,275 |

Where, SD = Standard deviation, CV = Coefficient of variation.

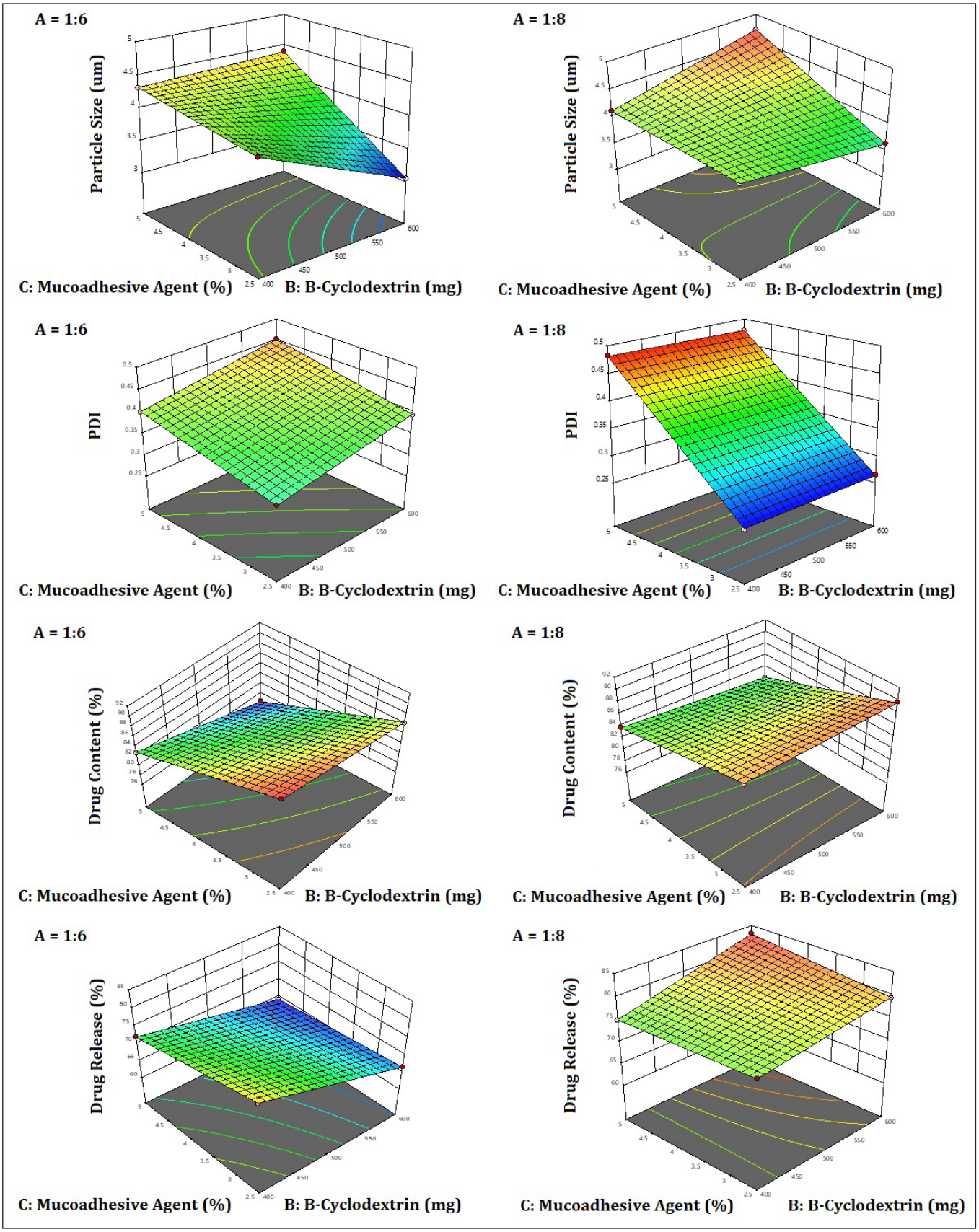


**Figure 8.** 3D surface plot showing the effect of independent variables on particle size, PDI, drug content, and drug release of remdesivir mucoadhesive DPI formulations.

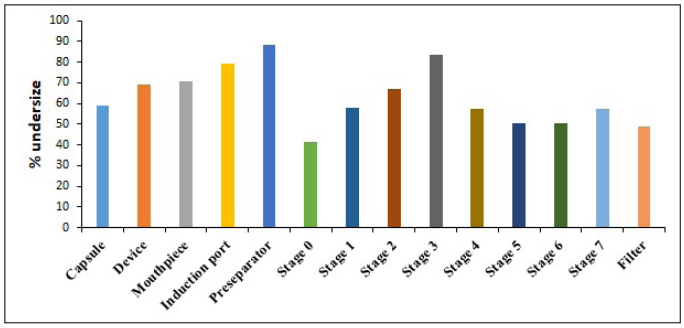


**Figure 9.** Aerodynamic diameter distribution of remdesivir mucoadhesive DPI formulation evaluated using ACI when emitted from Rotahaler.

**Table 8.** Results of stability study.

| Time period (days) | Particle size (um) | Polydispersity index | Drug content (%) | Drug release (%) |
|---|---|---|---|---|
| 0 | 3.642 ± 0.193 | 0.2,657 ± 0.0,169 | 89.73 ± 2.17 | 79.4 ± 2.2 |
| 30 | 3.661 ± 0.142 | 0.2,775 ± 0.0,174 | 89.48 ± 2.56 | 79.2 ± 2.1 |
| 60 | 3.692 ± 0.181 | 0.2,810 ± 0.0,158 | 89.43 ± 2.23 | 78.2 ± 2.4 |
| 90 | 3.701 ± 0.203 | 0.2,814 ± 0.0,165 | 89.35 ± 2.41 | 77.4 ± 1.5 |

Each value represents mean ± SD ($n$ = 3).

conditions for the preparation of dry powder [57,58]. The GSD was determined to be 0.950, signifying a small GSD, which suggests a narrow size distribution focused on smaller particle sizes. This combination of a low MMAD and a small GSD holds the potential for effective particle delivery, which can be advantageous.

*Stability study*

The stability investigation adhered to the ICH guidelines was conducted in order to assess the stability of the optimized batch of remdesivir mucoadhesive DPI. The parameters selected for the stability study were particle size, PDI, drug content %, and drug release %. The results of the stability study are illustrated in Table 8. After 30, 60, and 90 days, the sample was evaluated and there observed a very small change in all these parameters which indicated that the prepared remdesivir mucoadhesive DPI formulation was found to be stable.

## CONCLUSION

Remdesivir mucoadhesive DPI formulation was successfully formulated using a spray drying technique. The study results, including the obtained particle size (3.642 ± 0.193 µm), increased solubility (15–18 times higher), longer residence of the drug, and long-term stability, unequivocally demonstrate the significant potential of the remdesivir mucoadhesive DPI formulation for targeted drug delivery to the lungs, offering a viable alternative to traditional dosage forms. However, some variability in drug content was observed across different batches. In conclusion, the remdesivir mucoadhesive DPI formulated using a novel mucoadhesive agent (Samanea saman seed gum) represents a promising strategy for administering antiviral agents like remdesivir via the pulmonary route for localized action against pulmonary viral infections. However, the *in vivo* pharmacokinetic and pharmacodynamics studies are essential to further confirm the findings of the present study.

## LIST OF ABBREVIATIONS

ACI, Andersen cascade impactor; DPI, Dry powder inhalation; DSC, Differential scanning calorimetry; EBOV, Ebola virus; FPF, Fine particle fraction; FTIR, Fourier-transform infrared spectroscopy; GSD, Geometric standard deviation; HBoV, Human bocavirus; HMVE, Human umbilical vein endothelial; MERS-CoV, Coronavirus associated with middle east respiratory syndrome; MDI, Metered dose inhalers; MMAD, Mass median aerodynamic diameter; PCF, Pharyngoconjunctival fever; PDI, Polydispersity index; PBS, Phosphate buffer solution; SARS-CoV, Coronavirus associated with severe acute respiratory syndrome;

SEM, Scanning electron microscopy; UV, Ultra-violet; XRPD, X-ray powder diffraction.

## ACKNOWLEDGMENTS

The authors are grateful to AICTE, New Delhi, for providing a research grant (File No. 8-129/FDC/RPS/Policy-I/2021-22). The authors are sincerely thankful to RN Pharma Consulting, Pune, for their continuous guidance throughout the project and to Mylan R & D Centre, Bangalore, India, for generously supplying the gift sample of API remdesivir. The authors are also grateful to the management and principal of Marathwada Mitra Mandal's College of Pharmacy, Pune, for providing infrastructural support for the project.

## AUTHOR CONTRIBUTIONS

All authors made substantial contributions to conception and design, acquisition of data, or analysis and interpretation of data; took part in drafting the article or revising it critically for important intellectual content; agreed to submit to the current journal; gave final approval of the version to be published; and agree to be accountable for all aspects of the work. All the authors are eligible to be authors as per the International Committee of Medical Journal Editors (ICMJE) requirements/guidelines.

## CONFLICTS OF INTEREST

The authors report no financial or any other conflicts of interest in this work.

## ETHICAL APPROVALS

This study does not involve experiments on animals or human subjects.

## DATA AVAILABILITY

All data generated and analyzed are included in this research article.

## PUBLISHER'S NOTE

All claims expressed in this article are solely those of the authors and do not necessarily represent those of the those of the publisher, the editors and the reviewers. This

journal remains neutral with regard to jurisdictional claims in published institutional affiliation.

## USE OF ARTIFICIAL INTELLIGENCE (AI)-ASSISTED TECHNOLOGY

The authors declares that they have not used artificial intelligence (AI)-tools for writing and editing of the manuscript, and no images were manipulated using AI.

## REFERENCES


1. Lozano R, Naghavi M, Foreman K, Lim S, Shibuya K, Aboyans V, *et al.* Global and regional mortality from 235 causes of death for 20 age groups in 1990 and 2010: a systematic analysis for the Global Burden of Disease Study 2010. Lancet. 2012;380(9859):2095–128. doi: https://doi.org/10.1016/S0140-6736(12)61728-0
2. Boncristiani HF, Criado MF, Arruda E. Respiratory viruses. 3rd ed. In: Schaechter M, editor. Encyclopedia of microbiology. San Diego, CA: Academic Press; 2009. pp. 500–18. doi: https://doi.org/10.1016/b978-012373944-5.00314-x
3. Kinjo T, Fujita J. Differential diagnosis between influenza and other respiratory viral infections: What are the differential diagnoses? In: Fujita J, editor. Influenza. Respiratory disease series: diagnostic tools and disease management. Singapore: Springer; 2020. pp. 79–90. doi: https://doi.org/10.1007/978-981-15-9109-9_8
4. Siegel D, Hui HC, Doerffler E, Clarke MO, Chun K, Zhang L, *et al.* Discovery and synthesis of a phosphoramidate prodrug of a pyrrolo [2,1-f][triazin-4-amino] adenine C-nucleoside (GS-5734) for the treatment of ebola and emerging viruses. J Med Chem. 2017;60(5):1648–61. doi: https://doi.org/10.1021/acs.jmedchem.6b01594
5. Lo MK, Jordan R, Arvey A, Sudhamsu J, Shrivastava-Ranjan P, Hotard AL, *et al.* GS-5734 and its parent nucleoside analog inhibit filo-, Pneumo-, and Paramyxoviruses. Sci Rep. 2017;7(1):43395. doi: https://doi.org/doi:10.1038/srep43395
6. Ko WC, Rolain JM, Lee NY, Chen PL, Huang CT, Lee PI, *et al.* Arguments in favour of remdesivir for treating SARS-COV-2 infections. Int J Antimicrob Agents. 2020;55(4):105933. doi: https://doi.org/doi:10.1016/j.ijantimicag.2020.105933
7. Amirian ES, Levy JK. Current knowledge about the antivirals remdesivir (GS-5734) and GS-441524 as therapeutic options for Coronaviruses. One Health. 2020;9:100128. doi: https://doi.org/10.1016/j.onehlt.2020.100128
8. Warren TK, Jordan R, Lo MK, Ray AS, Mackman RL, Soloveva V, *et al.* Therapeutic efficacy of the small molecule GS-5734 against Ebola virus in Rhesus Monkeys. Nature. 2016;531(7594):381–5. doi: https://doi.org/10.1038/nature17180
9. Gordon CJ, Tchesnokov EP, Feng JY, Porter DP, Gotte M. The antiviral compound remdesivir potently inhibits RNA-dependent RNA polymerase from Middle East respiratory syndrome coronavirus. J Biol Chem. 2020;295(15):4773–9. doi: https://doi.org/10.1074/jbc.ac120.013056
10. Williamson BN, Feldmann F, Schwarz B, Meade-White K, Porter DP, Schulz J, *et al.* Clinical benefit of remdesivir in rhesus macaques infected with SARS-COV-2. Nature. 2020;585(7824):273–6; doi: https://doi.org/10.1038/s41586-020-2423-5
11. Deb S, Reeves AA, Hopefl R, Bejusca R. ADME and pharmacokinetic properties of Remdesivir: its drug interaction potential. Pharmaceuticals. 2021;14(7):655. doi: https://doi.org/10.3390/ph14070655
12. Bolger GT. Routes of drug administration. In: Riviere JE, Monteiro-Riviere NA, editors. Reference module in biomedical sciences. Amsterdam, The Netherlands: Elsevier; 2018. doi: https://doi.org/10.1016/b978-0-12-801238-3.11099-2
13. Borghardt JM, Kloft C, Sharma A. Inhaled therapy in respiratory disease: the complex interplay of pulmonary kinetic processes. Can Respir J. 2018;2018:1–11. doi: https://doi.org/10.1155/2018/2732017
14. Vermillion MS, Murakami E, Ma B, Pitts J, Tomkinson A, Rautiola D, *et al.* Inhaled remdesivir reduces viral burden in a nonhuman primate model of SARS-CoV-2 infection. Sci Transl Med. 2022;14(633):8282. doi: https://doi.org/10.1126/scitranslmed.abl8282
15. Zhang X, Liu Q, Hu J, Xu L, Tan W. An aerosol formulation of R-salbutamol sulfate for pulmonary inhalation. Acta Pharm Sin B. 2014;4(1):79–85. doi:http://doi.org/10.1016/j.apsb.2013.12.010
16. Rangaraj N, Pailla SR, Sampathi S. Insight into pulmonary drug delivery: mechanism of drug deposition to device characterization and regulatory requirements. Pulm Pharmacol Ther. 2019;54:1–21. doi: https://doi.org/10.1016/j.pupt.2018.11.004
17. Nguyen TT, Yi EJ, Hwang KM, Cho CH, Park CW, Kim JY, *et al.* Formulation and evaluation of carrier-free dry powder inhaler containing sildenafil. *Drug Deliv Transl Res*. 2018;9(1):319–33. doi: https://doi.org/10.1007/s13346-018-0586-5
18. Xiroudaki S, Ianni F, Sabbatini S, Roselletti E, Celi E, Vogias A, *et al.* Abstracts from the Aerosol Society drug delivery to the lungs 30 Edinburgh International Conference Centre Edinburgh, Scotland, UK December 11–13, 2019. J Aerosol Med Pulm Drug Deliv. 2020;33(2):A–1. doi: https://doi.org/10.1089/jamp.2020.ab01.abstracts
19. Shetty N, Cipolla D, Park H, Zhou QT. Physical stability of dry powder inhaler formulations. Expert Opin Drug Deliv. 2019;17(1):77–96. doi: https://doi.org/10.1080/17425247.2020.1702643
20. Woodcock A, Janson C, Rees J, Frith L, Lofdahl M, Moore A, *et al.* Effects of switching from a metered dose inhaler to a dry powder inhaler on climate emissions and asthma control: Post-hoc analysis. Thorax. 2022;77(12):1187–92. doi: https://doi.org/10.1136/thoraxjnl-2021-218088
21. Saldanha S, Fernandes B, Ventura J. Spray drying as an enabling technology for inhalation drug delivery. Pharm Technol. 2021;45(7):36–40.
22. Santos D, Mauricio AC, Sencadas V, Santos JD, Fernandes MH, Gomes PS. Spray drying: An overview. In: Pingatello R, Musumeci T, editors. Biomaterials - physics and chemistry—New Edition. IntechOpen; 2018. doi: https://doi.org/10.5772/intechopen.72247
23. Hoppentocht M, Hagedoorn P, Frijlink HW, de Boer AH. Technological and practical challenges of dry powder inhalers and formulations. Adv Drug Deliv Rev. 2014;75:18–31. doi: https://doi.org/10.1016/j.addr.2014.04.004
24. Baste NS, Basarkar GD. Samanea Saman: a novel mucoadhesive gum. Res J Pharmacogn Phytochem. 2021;13:57–62. doi: https://doi.org/10.52711/0975-4385.2021.00010
25. Tekade AR, Mathapati SU, Ratnaparkhi MP, Kulkarni GM. Bioavailability enhancement of poorly aqueous soluble atorvastatin calcium by solid dispersion technique using a modified natural polymer as a hydrophilic carrier. J Pharm Innov. 2023;18(4):2182–95. doi: https://doi.org/10.1007/s12247-023-09783-w
26. Devkar TB, Tekade AR, Khandelwal KR. Surface engineered nanostructured lipid carriers for efficient nose to brain delivery of ondansetron hcl using Delonix regia gum as a natural mucoadhesive polymer. Colloids Surf B: Biointerfaces. 2014;122:143–50. doi: https://doi.org/10.1016/j.colsurfb.2014.06.037
27. Patel M, Tekade A, Gattani S, Surana S. Solubility enhancement of lovastatin by modified locust bean gum using solid dispersion techniques. AAPS PharmSciTech. 2008;9(4):1262–9. doi: https://doi.org/10.1208/s12249-008-9171-4
28. Baste NS, Basarkar GD, Gangurde HH, Upasani CD. Design and development of oral mucoadhesive drug delivery system based on natural polymer. ECS Transactions. 2022;107(1):11239–59. doi: https://doi.org/10.1149/10701.11239ecst

29. Shingne NS, Nagpure SV, Deshmane SV, Biyani KR. Modified Hupu gum: a novel application in solid dispersion containing pioglitazone HCl. Am J PharmTech Res. 2013;3:463–72.
30. Alwossabi AM, Elamin ES, Ahmed EMM, Abdelrahman M. Solubility enhancement of some poorly soluble drugs by solid dispersion using Ziziphus spina-christi gum polymer. Saudi Pharm J. 2022;30(6):711–25. doi: https://doi.org/10.1016/j.jsps.2022.04.002
31. Rodde MS, Divase GT, Devkar TB, Tekade AR. Solubility and bioavailability enhancement of poorly aqueous soluble atorvastatin: *in vitro*, *ex vivo*, and *in vivo* studies. Biomed Res Int. 2014;2014:463895. doi: https://doi.org/10.1155/2014/463895
32. Jangra S, Ahuja M, Kumar A. Evaluation of mucoadhesive property of Gum Ghatti. J Pharm Investig. 2013;43(6):481–7. doi: https://doi.org/10.1007/s40005-013-0093-0
33. Nafee NA, Ismail FA, Boraie NA, Mortada LM. Mucoadhesive delivery systems. I. Evaluation of mucoadhesive polymers for buccal tablet formulation. Drug Dev Ind Pharm. 2004;30(9):985–93. doi: https://doi.org/10.1081/ddc-200037245
34. Brachet M, Arroyo J, Bannelier C, Cazals A, Fortun-Lamothe L. Hydration capacity: a new criterion for feed formulation. Anim Feed Sci Technol. 2015;209:174–85. doi: https://doi.org/10.1016/j.anifeedsci.2015.07.014
35. Murali Mohan Babu GV, Prasad ChDS, Ramana Murthy KV. Evaluation of modified Gum Karaya as carrier for the dissolution enhancement of poorly water-soluble drug nimodipine. Int J Pharm. 2002;234(1–2):1–17. doi: https://doi.org/10.1016/s0378-5173(01)00925-5
36. Bhagwat DA, Kolekar VR, Nadaf SJ, Choudhari PB, More HN, Killedar SG. Acrylamide grafted neem (Azadirachta indica) gum polymer: screening and exploration as a drug release retardant for tablet formulation. Carbohydr Polym. 2020;229:115357. doi: https://doi.org/10.1016/j.carbpol.2019.115357
37. Mahajan HS, Gundare SA. Preparation, characterization and pulmonary pharmacokinetics of Xyloglucan microspheres as dry powder inhalation. Carbohydr Polym. 2014;102:529–36. doi: https://doi.org/10.1016/j.carbpol.2013.11.036
38. Saha T, Sinha S, Harfoot R, Quinones-Mateu ME, Das SC. Inhalable dry powder containing remdesivir and disulfiram: preparation and *in vitro* characterization. Int J Pharm. 2023;645:123411. doi: https://doi.org/10.1016/j.ijpharm.2023.123411
39. Manconi M, Nacher A, Merino V, Merino-Sanjuan M, Manca ML, Mura C, *et al.* Improving oral bioavailability and pharmacokinetics of liposomal metformin by glycerolphosphate–chitosan microcomplexation. AAPS PharmSciTech. 2013;14(2):485–96. doi: https://doi.org/10.1208/s12249-013-9926-4
40. LeClair DA, Cranston ED, Xing Z, Thompson MR. Optimization of spray drying conditions for yield, particle size and biological activity of thermally stable viral vectors. Pharm Res. 2016;33(11):2763–76. doi: https://doi.org/10.1007/s11095-016-2003-4
41. Saha T, Sinha S, Harfoot R, Quinones-Mateu ME, Das SC. Spray-dried inhalable microparticles combining remdesivir and ebselen against SARS-CoV-2 infection. Pharmaceutics. 2023;15:2229. doi: https://doi.org/10.3390/pharmaceutics15092229
42. Alqaheem Y, Alomair AA. Microscopy and spectroscopy techniques for characterization of polymeric membranes. Membranes. 2020;10(2):33. doi: https://doi.org/10.3390/membranes10020033
43. Tekade AR, Suryavanshi MR, Shewale AB, Patil VS. Design and development of donepezil hydrochloride loaded nanostructured lipid carriers for efficient management of Alzheimer's disease. Drug Dev Ind Pharm. 2023;49(9):590–600. doi: https://doi.org/10.1080/03639045.2023.2262035
44. Dolega A, Juszynska-Galazka E, Osiecka-Drewniak N, Natkanski P, Kustrowski P, Krupa A, *et al.* Study on the thermal performance of carbamazepine at different temperatures, pressures and atmosphere conditions. Thermochimica Acta. 2021;703:178990. doi: https://doi.org/10.1016/j.tca.2021.178990
45. Pardeshi CV, Rajput PV, Belgamwar VS, Tekade AR. Formulation, optimization and evaluation of spray-dried mucoadhesive microspheres as intranasal carriers for Valsartan. J Microencapsul. 2011;29(2):103–14. doi: https://doi.org/10.3109/02652048.2011.630106
46. Sahakijpijarn S, Moon C, Koleng JJ, Christensen DJ, Williams RO. Development of remdesivir as a dry powder for inhalation by thin film freezing. Pharmaceutics. 2020;12(11):1002. doi: https://doi.org/10.3390/pharmaceutics12111002
47. Jadhav K, Dhamecha D, Tate A, Tambe H, Patil MB. Application of UV spectrophotometric method for easy and rapid estimation of lafutidine in bulk and pharmaceutical formulation. Pharm Methods. 2011;2(4):264–7. doi: https://doi.org/10.4103/2229-4708.93398
48. Belgamwar VS, Patel HS, Joshi AS, Agrawal A, Surana SJ, Tekade AR. Design and development of nasal mucoadhesive microspheres containing tramadol HCl for CNS targeting. Drug Deliv. 2011;18(5):353–60. doi: https://doi.org/10.3109/10717544.2011.557787
49. Lewis D, Copley M. Inhaled product characterization: calculating particle-size distribution metrics. Pharm Technol. 2011;2011(6):S33–S7.
50. Ratnaparkhi MP, Kamble OV, Salvankar SS, Shinde SR, Kulkarni GM, Shewale AB, *et al.* Formulation and evaluation of moxifloxacin dry powder inhaler combined with mucolytic agent for pulmonary diseases. *Int J Drug Deliv Technol.* 2023;13(3):818–24. doi: https://doi.org/10.25258/ijddt.13.3.07
51. Williams TR. Infrared absorption spectroscopy. J Chem Educ. 1963;40(11):616. doi: https://doi.org/10.1021/ed040p616.3
52. Great Britain. Medicines Commission. British Pharmacopoeia. London, UK: The Stationery Office; 2001. vol 1. p. 20–3.
53. Kirk J, Dann S, Blatchford C. Lactose: a definitive guide to polymorph determination. Int J Pharm. 2007;334(1–2):103–14. doi: https://doi.org/10.1016/j.ijpharm.2006.10.026
54. Norris KP, Greenstreet JE. Infra-red absorption spectra of casein and lactose. Nature. 1958;181(4604):265–6. doi: https://doi.org/10.1038/181265b0
55. Pouchert CJ. Aldrich Library of FT-IR spectra. 1st ed. St. Louis, MO: Aldrich Chemical Company; 1985. pp. 279–396.
56. Laucks ML. Aerosol technology properties, behavior, and measurement of airborne particles. J Aerosol Sci. 2000;31:1121–2. doi: https://doi.org/10.1016/s0021-8502(99)00571-6
57. Wong SN, Low KH, Poon YL, Zhang X, Chan HW, Chow SF. Synthesis of the first remdesivir cocrystal: design, characterization, and therapeutic potential for pulmonary delivery. Int J Pharm. 2023;640:122983. doi: https://doi.org/10.1016/j.ijpharm.2023.122983
58. Chan HW, Lee HK, Chow S, Lam DL, Chow SF. Integrated continuous manufacturing of inhalable remdesivir nanoagglomerate dry powders: design, optimization and therapeutic potential for respiratory viral infections. Int J Pharm. 2023;644:123303. doi: https://doi.org/10.1016/j.ijpharm.2023.123303


**How to cite this article:**
Ratnaparkhi MP, Kulkarni GM, Salvankar SS, Tekade AR. Development and evaluation of Remdesivir dry powder inhalation formulation by spray drying technique. J Appl Pharm Sci. 2025;15(02):127–141.